Hindawi
Journal of Food Biochemistry
Volume 2023, Article ID 8883860, 17 pages
https://doi.org/10.1155/2023/8883860

Research Article

Study on Antipyretic Properties of Phenolics in Lonicerae Japonicae Flos Based on Ultrahigh Performance Liquid Chromatography-Tandem Mass Spectrometry Combined with Network Pharmacology

Lewen Xiong,[1] **Wenjing Huang**,[2] **Yan Liu**,[1] **Hongwei Zhao**,[1] **Yang Wang**,[1] **Ying Jin**,[1] **Longfei Zhang**,[1] **and Yongqing Zhang**[1]

[1]*School of Pharmacy, Shandong University of Traditional Chinese Medicine, Jinan 250355, China*
[2]*Weifang Traditional Chinese Medicine Hospital, Weifang, China*

Correspondence should be addressed to Longfei Zhang; longfei_zhang@sdutcm.edu.cn

Received 5 July 2023; Revised 12 October 2023; Accepted 24 November 2023; Published 8 December 2023

Academic Editor: Muhammad Babar Khawar

Copyright © 2023 Lewen Xiong et al. This is an open access article distributed under the Creative Commons Attribution License, which permits unrestricted use, distribution, and reproduction in any medium, provided the original work is properly cited.

Objective. To identify and quantify the active phenolic components in Lonicerae japonicae flos (LJF) for fever treatment and their mechanism of action using network pharmacology and molecular docking. *Methods*. Based on qualitative analysis of LJF, 194 phenolics were obtained, including 81 phenolic acids and 113 flavonoids. Gene Ontology and Kyoto Encyclopedia of Genes and Genomes pathway analyses were used to identify potential targets for these components to interact with fever. Molecular docking with microsomal PGE2 synthase-1, EP1, EP2, EP3, and EP4 targets was used to determine antipyretic components. The antipyretic efficacy of the main components was verified by in vivo experiments. Finally, high-performance liquid chromatography-tandem mass spectrometry was used to quantify the main antipyretic components of LJF. *Results*. Phenolics in LJF may prevent and treat fever by participating in calcium signaling, regulating TRP channels, and cAMP signaling. Luteolin-7-*O*-glucoside, apigenin-7-*O*-glucoside, 3,5-*O*-dicaffeoylquinic acid, luteolin, and other components have a good docking effect with PGE2 synthase-1 and its four subtypes. 3,5-*O*-dicaffeoylquinic acid, luteolin-7-*O*-glucoside, and apigenin-7-*O*-glucoside have good antipyretic effects in a yeast-induced pyrexia model. The content of these antipyretic components varies with the developmental period of LJF. Phenolic acids are the main components that distinguish the different developmental periods of LJF. *Conclusion*. The potential antipyretic components and molecular mechanisms of phenolics provide a basis for the traditional medicinal effects and future development and utilization of LJF.

1. Introduction

Lonicerae japonicae flos (LJF), the flower buds of *Lonicera japonica* Thunb. (LJT), is a traditional Chinese medicine used for medicine and food, with potential antipyretic and anti-inflammatory activities [1]. It was used to treat various diseases, including exopathogenic wind-heat, epidemic febrile diseases, sores, carbuncles, and infectious diseases [2]. The LJF has a complex chemical component with phenolic acids, flavonoids, iridoids, volatile oils, and triterpenoid saponins [3]. Phenolic acids have antiviral [4, 5], antibacterial [6, 7], anti-inflammatory [8, 9], antitumor [10], and medicinal activities. These activities are related to the traditional efficacy of LJF, as shown by modern pharmacological studies. Phenolic acids are the primary medicinal substances of LJF. The 2000 edition of the "Chinese Pharmacopoeia" established the content of chlorogenic acid as the quality control index of LJT, with a minimum requirement of 1.5% [11]. The 2020 edition of the "Chinese Pharmacopoeia" increased the quality standards of LJT by increasing the content index of phenolic acid components, including chlorogenic acid, 3,5-*O*-dicaffeoylquinic acid, and

4,5-*O*-dicaffeoylquinic acid, which should not be less than 3.8% in total [1, 12]. Flavonoids in LJT have various antibacterial [13, 14], anti-inflammatory [15, 16], antioxidant [17], antitumor [18, 19], and neuroprotective [20, 21] effects. According to Chinese Pharmacopeia, luteolin-7-*O*-glucoside in flavonoids is used as an evaluation and control index for the quality of LJF [1]. Phenolic acids and flavonoids are both phenolics. Therefore, phenolics in LJF deserve extensive attention.

Fever is a common symptom of infectious and inflammatory disease. Prostaglandin E2 is the final mediator of fever. Inflammatory stimulation may induce fever by activating cyclooxygenase-2 and microsomal PGE synthase in brain endothelial cells [22–24] or perivascular cells [25]. Simultaneously, brain-bound cells release PGE2, which causes fever by affecting neurons expressing the EP receptor [26, 27]. Microsomal PGE2 synthase-1 (mPGES-1) is considered a key target for developing new anti-inflammatory drugs due to its association with various human diseases and pathological states, including pain, fever, and rheumatoid arthritis [28]. Hence, mPGES-1 presents a crucial target protein in the pursuit of antipyretic drugs. Additionally, the PGE receptors exhibit four distinct subtypes, namely, EP1, EP2, EP3, and EP4, each performing a unique function in the acute phase response of fever [29–32]. For instance, activation of EP4 receptors escalates cAMP levels, whereas activation of the EP1 receptor boosts intracellular Ca^{2+} levels, and activation of the EP3 receptor either diminishes or augments cAMP levels based on its isoform [33, 34]. Consequently, EP receptors are intimately associated with fever and could potentially offer an avenue to regulate it.

This study explored the antipyretic mechanism of phenolics in LJF using network pharmacology. Molecular docking was conducted between LJF components and fever-related targets, including mPGES-1, EP1, EP2, EP3, and EP4. In vivo experiments were used to verify the main antipyretic components and quantify those using ESI-QqQ-MS/MS. These findings provide a scientific explanation for LJF's traditional heat-clearing and detoxifying effects and can be used as a reference for quality control. The research process is shown in Figure 1.

2. Materials and Methods

2.1. Network Pharmacology of Phenolic Components of LJF [35]

2.1.1. Analysis of the Phenolic Components of LJF. The phenolics of LJF were identified by preliminary experiments and used as the component database of LJF.

2.1.2. Potential Target Mining. Targets of active components were predicted by the SwissTargetPrediction database (https://www.swisstargetprediction.ch/). With "fever," "febrile," and "heat" as keywords, the DrugBank database (https://go.drugbank.com/), GeneCards database (https://www.genecards.org/), and TTD database (https://db.idrblab.net/ttd/) were used to retrieve disease targets.

The potential targets of LJF for the treatment of fever were obtained by repeatedly screening the disease targets and the predicted targets of potential active components. The potential targets and their related components imported Cytoscape 3.7.1 software and built a multivariate network.

2.1.3. Gene Ontology (GO) Analysis and Kyoto Encyclopedia of Genes and Genomes (KEGG) Pathway Analysis. The Metascape website (https://metascape.org) [36] and the KEGG database (https://www.kegg.jp/) [37] were used for GO analysis and KEGG pathway analysis of potential targets.

2.1.4. Molecular Docking. Data for MPGES1 (PDB ID: 4AL0), EP1 (Uniprot ID: P34995), EP2 (PDB ID: 7CX2), EP3 (PDB ID: 6M9T), and EP4 (PDB ID: 5YWY) were downloaded from the RSCB database (https://www.rcsb.org/) and the UniProt database (https://www.uniprot.org/). PyMOL 1.7.2.1 software was used to extract the 3D structure of the target protein. The structure was optimized using AutoDock Tools 1.5.6 software and then stored in PDBQT format. The molecular docking grid was set as surrounding residues centered on the primary ligand of the target protein. AutoDock Vina 1.1.2 and Python scripts were used to conduct molecular docking and to record and sort the binding energies.

2.2. In Vivo Experiment of Antipyretic Effects

2.2.1. Chemicals and Materials. Yeast (Saccharomyces cerevisiae) was purchased from Angel Yeast Co., Ltd. (Hubei, China). Paracetamol injection was obtained from Chenxin Pharmaceutical Co., Ltd. (Jining, China). HH801B high-accuracy thermocouple thermometers were purchased from Omega Engineering (Shanghai, China). PGE2, IL-6, TNF-α, and IL-1β ELISA kits were provided by Shanghai Enzyme Linked Biotechnology Co., Ltd. (Shanghai, China).

2.2.2. Animals and Ethics Statement. C57BL/6N mice (male, 8 weeks) were purchased from Beijing Vital River Laboratory Animal Technology Co., Ltd. (Beijing, China). Mice were maintained in the SPF Laboratory Animal Center of the Shandong University of Traditional Chinese Medicine (SDUTCM). The animals were maintained at constant room temperature ($25 \pm 2^{\circ}C$) on a 12 h light/dark cycle with free access to food and water for 24 h or more before experiments. All experiments were performed in accordance with international guidelines and approved by the animal ethics committee of SDUTCM (No. YYLW2023000011).

2.2.3. Drugs Preparation. Low dose (10 mg/kg) and high dose (50 mg/kg) of 3,5-*O*-dicaffeoylquinic acid were prepared. Low dose (20 mg/kg) and high dose (80 mg/kg) of luteolin-7-*O*-glucoside and apigenin-7-*O*-glucoside were prepared, respectively. The positive drug (paracetamol injection) was 2 mL (0.25 g), and the dose was 100 mg/kg. Yeast powder was dissolved in normal saline to prepare 20% yeast suspension and incubated at $37^{\circ}C$ for 30 min.

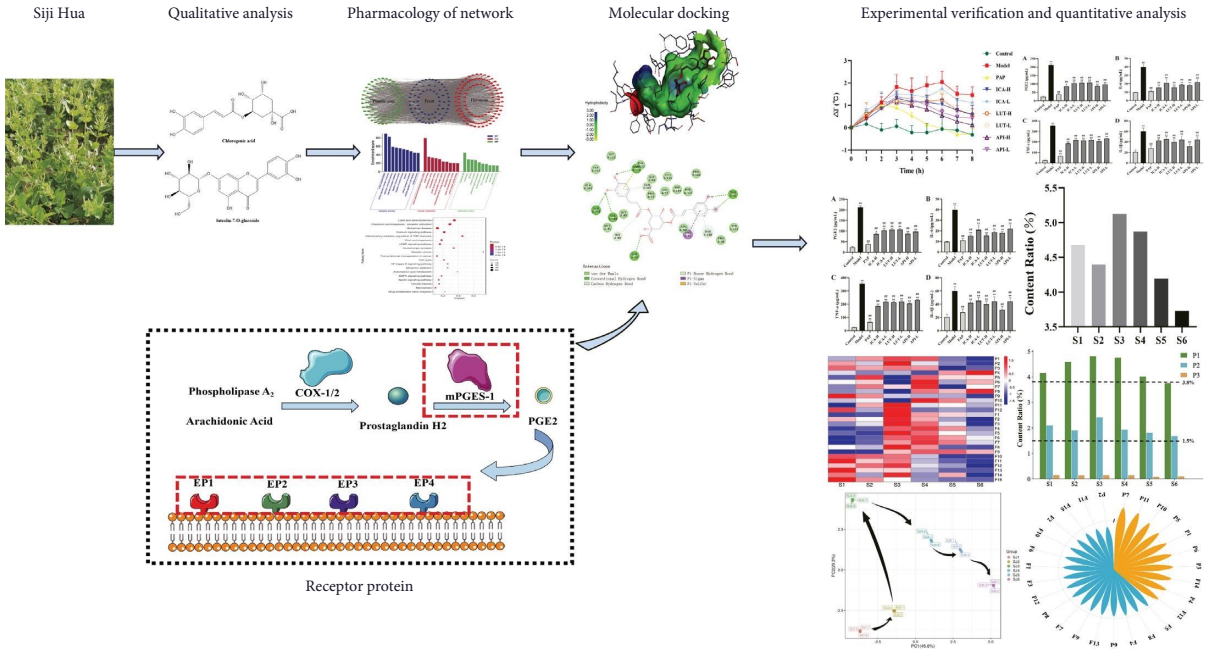

Figure 1: Research and analysis flowchart.

2.2.4. Antipyretic Activity Test. The base rectal temperature of each animal was measured by a thermometer in the rectum before the yeast injection. Mice with a base rectal temperature of 36.5–37.5°C were selected for antipyretic assays. 20% aqueous suspension of yeast was injected subcutaneously behind the neck of the animal (10 mL/kg) [38, 39]. The body temperature of the mice increased by >0.5°C at 5 h after injection, which was recognized as successfully prepared, and the temperature at this time was recorded as T0 (°C). Mice groups (9 groups of 5 mice each) were administered with their respective drugs. The intraperitoneal injection was performed in all groups. The temperatures (Ti, °C) were recorded after the administration of the drugs. After 8 h of mice body temperature determination, ΔT (Ti-T0, °C), mouse serum was collected.

2.3. Quantitative Study on Antipyretic Components Instruments

2.3.1. Materials and Reagents. Chlorogenic acid, 3,5-*O*-dicaffeoylquinic acid, 4,5-*O*-dicaffeoylquinic acid, protocatechuic acid, chlorogenic acid methyl ester, 5-*O*-caffeoylquinic acid, 4-*O*-caffeoylquinic acid, 3,4-*O*-dicaffeoylquinic acid, caffeic acid, ferulic acid, quercetin-3-*O*-rutinoside, isoquercitrin, luteolin-7-*O*-glucoside, luteolin-7-*O*-neohesperidoside, kaempferol-3-*O*-rutinoside, kaempferol-3-*O*-glucoside, isorhamnetin-3-*O*-glucoside, apigenin-7-*O*-glucoside, tricin-7-*O*-glucoside, luteolin, quercetin, diosmetin, apigenin, and tricin were purchased from Shanghai Yuanye Bio-Technology Co., Ltd. (Shanghai, China). 3,5-*O*-dicaffeoylquinic acid methyl ester and caffeic acid ethyl ester were purchased from Yunnan Xili Biotechnology Co., Ltd. (Yunnan, China). Quercetin-3-*O*-galactoside was purchased from ChemFaces Biochemical Co., Ltd. (Hubei, China). The purities of all reference standards is above 98%. Methanol, acetonitrile, and phosphoric acid were HPLC grade and obtained from Fisher Corporation (Waltham, MA, USA).

The LJF samples were collected from the medicinal botanical garden of Shandong University of Traditional Chinese Medicine (the germplasm is "Siji Hua"). The samples were divided into 6 periods (S1–S6) [40]. All dried material was ground to 65 mesh by liquid nitrogen.

2.3.2. Apparatus. The KQ-500DE digital ultrasonic cleaning instrument was purchased from Henan Brother Instruments Co., Ltd. (Zhengzhou, China). A ME204/02 Precision electronic balance was purchased from Mettler-Toledo Instruments Co., Ltd. (Shanghai, China).

Chromatographic analysis was performed on an Agilent 1290 series UPLC system (Agilent Technologies, Santa Clara, CA, USA). Mass spectrometry detection was performed using an Agilent 6460 series triple-quadrupole tandem mass spectrometer (QqQ-MS/MS) (Agilent Technologies, Santa Clara, CA, USA).

2.3.3. Quantitative Experimental Method. The preparation of samples, preparation of solutions, analysis methods, and method validation were referenced in previous studies [40, 41]. The information and HPLC-MS/MS parameters for MRM on phenolic acids and flavonoids are shown in Supplementary Table 1.

2.4. Statistical Analysis. All values were presented as mean ± S.D. Statistical analysis was performed using a one-way analysis of variance (ANOVA) model by SPSS 21.0. PCA and OPLS-DA were carried out by SIMCA software 14.1 version.

3. Results

3.1. The Phenolic Components of LJF. In total, 194 phenolics of LJF were identified, including 81 phenolic acids and 113 flavonoids. These active components are summarized in Supplementary Table 2. The MS chromatogram is shown in Supplementary Figure 1.

3.2. Target Mining. From the DrugBank database, GeneCards database, and TDD database, 11103 targets associated with fever were retrieved. 853 predicted targets for phenolic components of LJF were obtained. After the repeated screening, 586 potential targets were obtained. By taking the phenolic components directly related to potential targets as nodes, a multicomponent network was constructed (Figure 2). The figure contains 78 phenolic acids and 108 flavonoids, which are closely related to fever.

3.3. GO Analysis. 586 potential targets were subjected to GO cluster analysis. It mainly included biological process (BP), molecular function (MF), and cell composition (CC). According to the P value of GO enrichment analysis to filter results (Figure 3), BP is mainly involved in protein phosphorylation. CC mainly involves membrane rafts, and MF mainly involves protein serine/threonine/tyrosine kinase activity.

3.4. KEGG Pathway Analysis. Overall, 586 potential targets received 252 pathways. The top 15 pathways were selected for visual analysis using gene number, P value, and gene ratio as study parameters (Figure 4).

Among them, lipid and atherosclerosis, chemical carcinogenesis-receptor activation, calcium signaling pathway, inflammatory mediator regulation of TRP channels, cAMP signaling pathway, and NF-kappa B signaling pathway were closely related to fever and inflammation.

3.5. Molecular Docking. Molecular docking was performed between the 194 potential antipyretic components of LJF and the target proteins. Molecular docking results showed that the binding energies of the 194 potential antipyretic components with five kinds of protein were all less than 0.

The docking binding energies of each component and the five proteins were summed and sorted (Figure 5). 3,5-*O*-dicaffeoylquinic acid had the best docking and binding energy with mPGES-1, EP1, and EP4, with the value of −7.0, −9.8, and −10.0, respectively. The binding energy of luteolin-7-*O*-glucoside and EP2 was the best, which was −10.3, whereas, for EP3 binding, apigenin-7-*O*-glucoside and EP3 presented the best binding energy, with a value of −10.8. The potential antipyretic component and the amino acid residues of the target protein in the binding site mainly undergo hydrophobic binding via pi-cation, pi-alkyl, pi-donor hydrogen bond, pi-sigma, pi-sulfur, pi-pi-T-shaped, van der Waals, carbon-hydrogen bond, and conventional hydrogen bond interactions. These interactions increased the binding between the target protein and the active component.

The components with good binding energy and suitable for quantitative determination are summarized in Table 1. The results showed that luteolin-7-*O*-glucoside, apigenin-7-*O*-glucoside, 3,5-*O*-dicaffeoylquinic acid, and luteolin had the best binding energy.

3.6. Three Components Exert Antipyretic Effect during Yeast-Induced Fever. To observe the impact of three components on thermoregulatory responses during yeast-induced fever, recordings of ΔT (°C) were conducted for 8 hours after administration of the components (Figure 6). Results indicated no significant difference between the control and the PAP groups or the control groups and API-H groups. However, there were significant differences between the control and other groups ($P < 0.01$), demonstrating that PAP and API-H groups have superior antipyretic effects. Significant differences were observed between the model group and other groups at the partial time node, indicating that both high and low doses of the three components possess antipyretic effects.

3.7. Effect of Three Components on the Levels of Endogenous Pyrogen and Febrile Mediator. PGE2, IL-6, TNF-α, and IL-1β are endogenous pyrogen or febrile mediators that play key roles in the fever response [42, 43]. The present study evaluated the effect of three components on the levels of PGE2, IL-6, TNF-α, and IL-1β in the yeast-induced fever mice with paracetamol as a positive control. As shown in Figure 7, compared with the control without yeast injection, the plasma levels of PGE2, IL-6, TNF-α, and IL-1β of yeast-induced fever mice were markedly increased. The differences were statistically significant ($P < 0.01$). However, these three components inhibited the yeast-induced increase in PGE2, IL-6, TNF-α, and IL-1β in the plasma.

3.8. Validation of Methodology. The investigation found that all components had repeatability RSD of ≤3.02%, intraday precision RSD of ≤3.17%, interday precision RSD of ≤3.44%, stability within 48 h of ≤3.47%, and recovery RSD of ≤3.05%. The sample recovery ranged from 92.80% to 107.40%. The validation results are presented in Table 2.

3.9. Changes of Component Contents in Different Developmental Periods of LJF

3.9.1. Change of Antipyretic Components in LJF. The phenolic acids and flavonoids in LJF at different developmental periods are presented in Supplementary Table 3. The content changes of the four components with the best binding energy are shown in Figure 8. F4 (luteolin-7-*O*-glucoside) and F9 (apigenin-7-*O*-glucoside) had increased and decreased content, reaching a peak in the S4 period; P2 (3,5-*O*-dicaffeoylquinic acid) reached its peak in S3 period, and F11 (quercetin) showed a gradual decline. Interestingly, 3,5-*O*-dicaffeoylquinic acid and apigenin-7-*O*-glucoside were quality control components of LJF in Chinese Pharmacopoeia. These two components partly reflect the antipyretic effect of LJF, which has clinical significance.

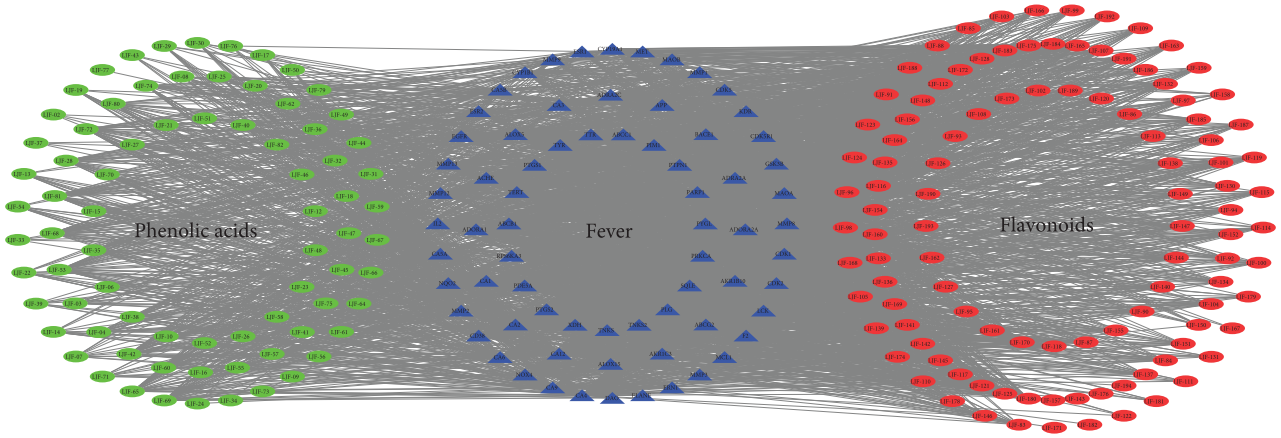

Figure 2: "Potential components and potential targets" network.

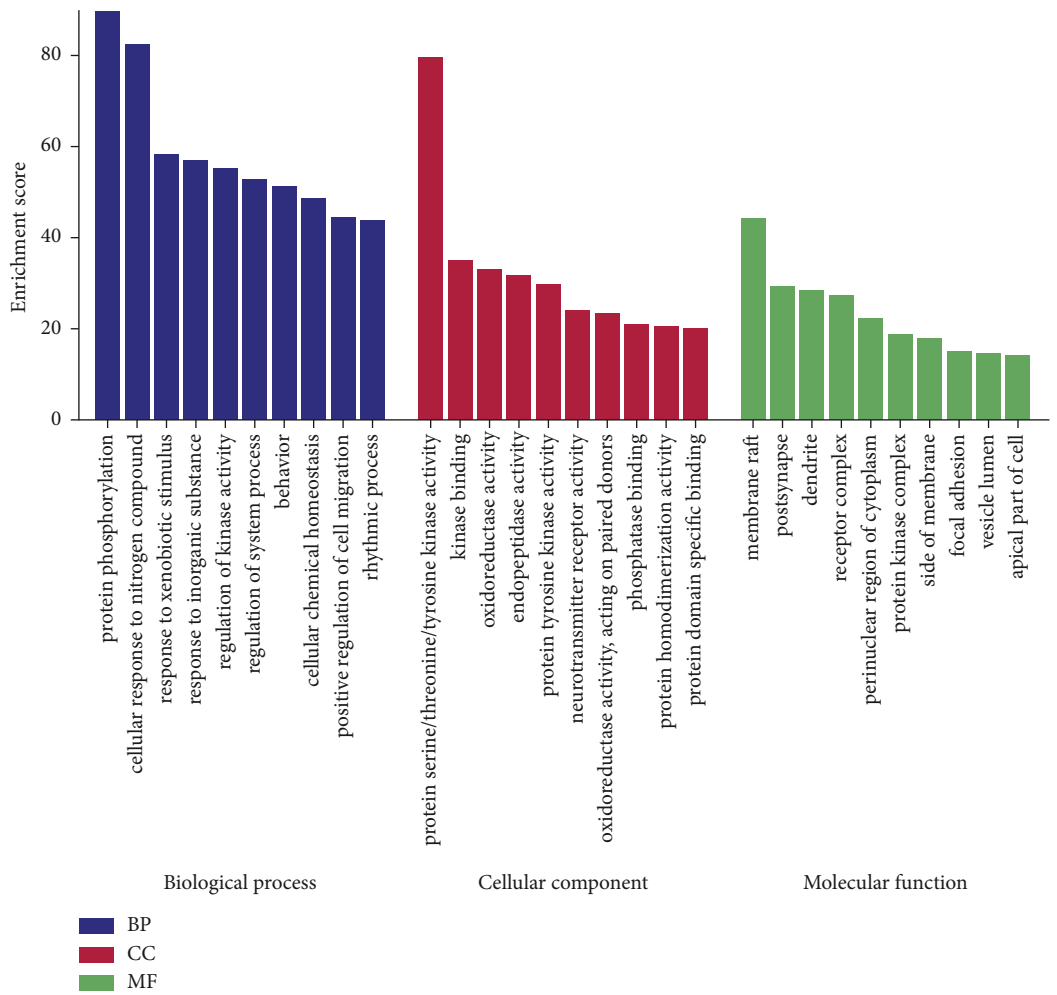

Figure 3: GO enrichment analysis diagram.

The study found that chlorogenic acid comprised 68% of the total component content. To avoid high-content components affecting trace components, the content ratio of different components in different developmental periods was analyzed (Figure 9). The figure showed that the total proportion of each component increased and then decreased with the developmental period. This change can reflect the distribution of each component's content and indirectly reflect the antipyretic effect of LJF in different periods. A higher total proportion of components resulted in a better antipyretic effect.

Although the overall phenolics demonstrated effective antipyretic properties during the S3 and S4 periods, the

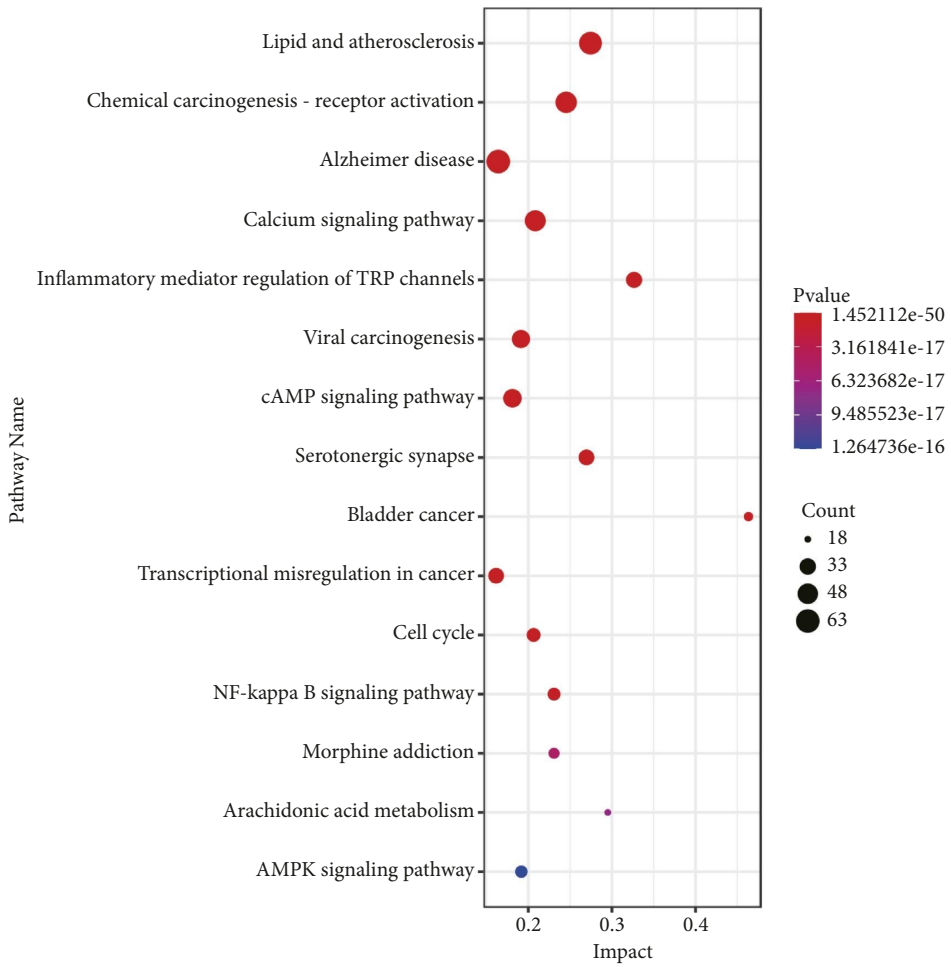

Figure 4: KEGG pathway enrichment analysis bubble chart.

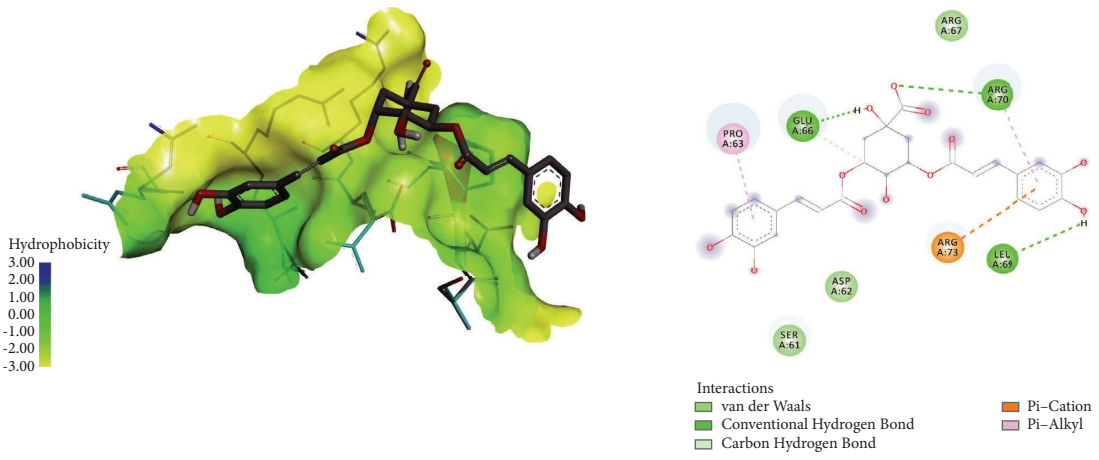

(a) (b)

Figure 5: Continued.

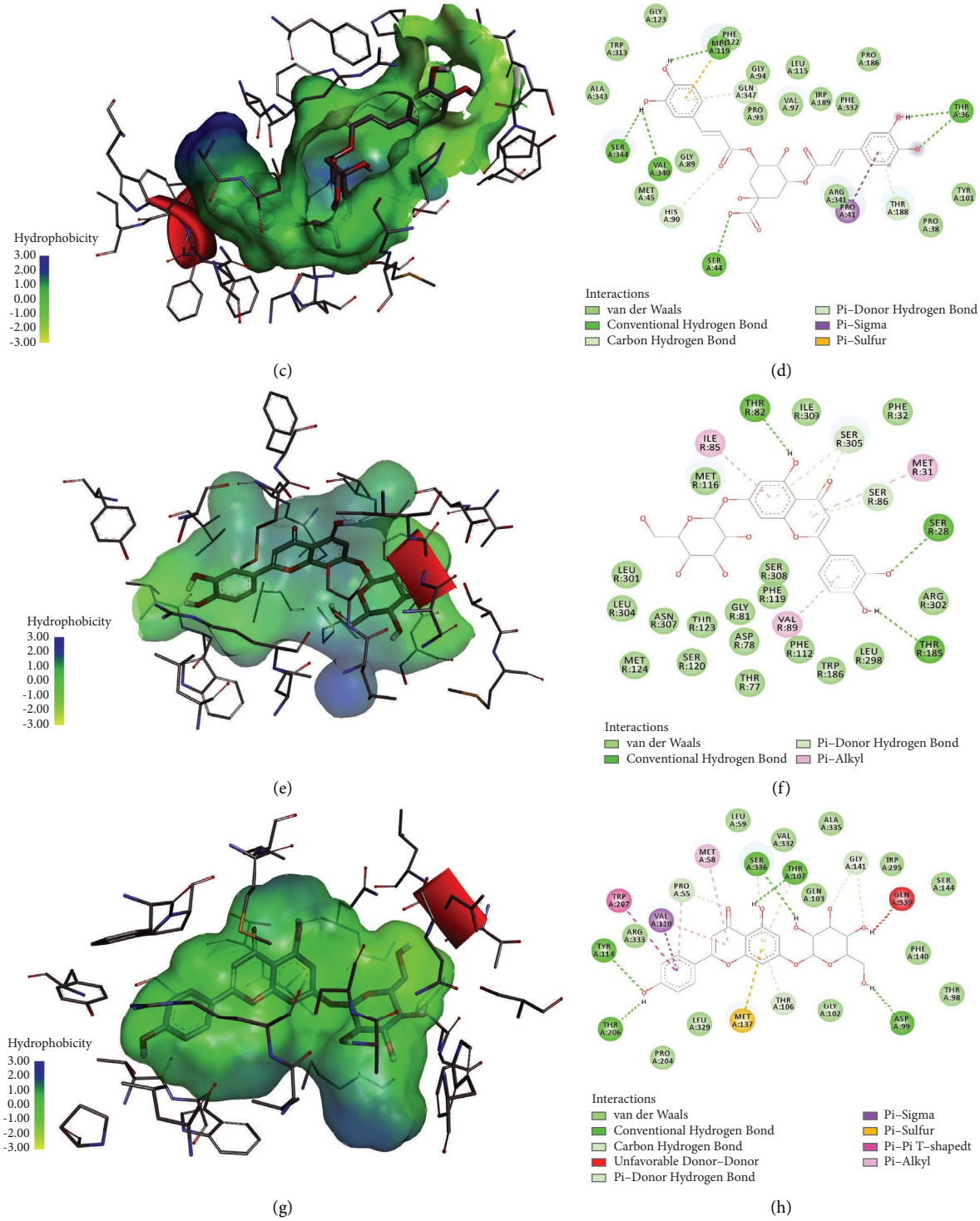

Figure 5: Continued.

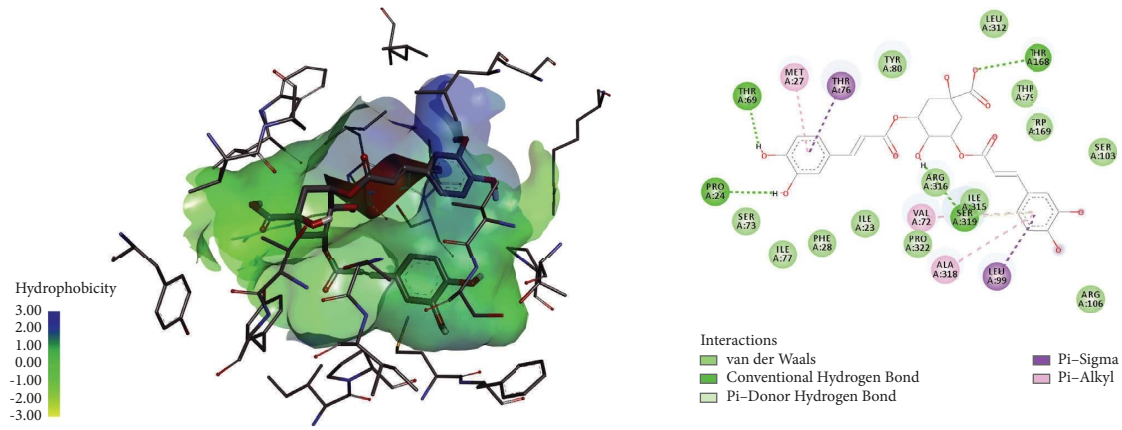

(i) (j)

Figure 5: mPGES-1 and 3,5-*O*-dicaffeoylquinic acid molecular docking 3D and 2D images (a, b); EP1 and 3,5-*O*-dicaffeoylquinic acid molecular docking 3D and 2D images (c, d); EP2 and luteolin-7-*O*-glucoside molecular docking 3D and 2D images (e, f); EP3 and apigenin-7-*O*-glucoside molecules docking 3D and 2D images (g, h); EP4 and 3,5-*O*-dicaffeoylquinic acid molecules docking 3D and 2D images (i, j).

Table 1: Binding energy of quantitative components.

No.	Name	Binding energy					
		mPGES-1	EP1	EP2	EP3	EP4	Total
P1	Chlorogenic acid	−5.7	−8.0	−8.4	−8.8	−8.2	−39.1
P2	3,5-*O*-Dicaffeoylquinic acid	−7.0	−9.8	−8.7	−8.2	−10.0	−43.7
P3	4,5-*O*-Dicaffeoylquinic acid	−6.6	−6.2	−8.9	−8.4	−9.6	−39.7
P4	3,4-Dihydroxybenzoic acid	−4.9	−5.7	−5.8	−5.9	−5.8	−28.1
P5	Methyl caffeate	−5.2	−5.9	−6.2	−6.3	−6.0	−29.6
P6	Chlorogenic acid methyl ester	−5.8	−7.8	−8.6	−8.3	−8.1	−38.6
P7	5-*O*-Caffeoylquinic acid	−6.2	−8.1	−8.9	−8.8	−8.8	−40.8
P8	4-*O*-Caffeoylquinic acid	−5.7	−8.0	−8.8	−9.1	−8.3	−39.9
P9	3,4-*O*-Dicaffeoylquinic acid	−5.4	−7.2	−9.0	−7.9	−9.3	−38.8
P10	Caffeic acid	−5.1	−5.9	−6.4	−6.7	−6.2	−30.3
P11	Ferulic acid	−5.1	−5.7	−6.2	−6.4	−6.1	−29.5
P12	3,5-*O*-Dicaffeoylquinic acid methyl ester	−6.9	−7.4	−8.0	−8.2	−9.9	−40.4
F1	Quercetin-3-*O*-rutinoside	−6.4	−8.5	−7.6	−5.3	−8.2	−36.0
F2	Quercetin-3-*O*-galactoside	−5.6	−7.6	−8.6	−7.3	−8.5	−37.6
F3	Isoquercitrin	−6.1	−6.3	−8.1	−7.7	−8.8	−37.0
F4	Luteolin-7-*O*-glucoside	−6.4	−9.5	−10.3	−10.4	−9.8	−46.4
F5	Luteolin-7-*O*-neohesperidoside	−6.6	−7.3	−6.2	−7.7	−7.6	−35.4
F6	Kaempferol-3-*O*-rutinoside	−6.3	−7.3	−8.1	−5.3	−9.4	−36.4
F7	Kaempferol-3-*O*-glucoside	−6.0	−8.7	−8.4	−7.2	−8.8	−39.1
F8	Isorhamnetin-3-*O*-glucoside	−5.7	−6.8	−7.7	−6.7	−8.9	−35.8
F9	Apigenin-7-*O*-glucoside	−6.8	−6.9	−10.0	−10.8	−9.5	−44.0
F10	Tricin-7-*O*-glucoside	−5.9	−6.6	−9.3	−8.8	−8.4	−39.0
F11	Luteolin	−6.3	−8.3	−9.0	−9.0	−8.6	−41.2
F12	Quercetin	−6.0	−8.2	−9.0	−8.6	−8.3	−40.1
F13	Diosmetin	−5.8	−8.0	−9.0	−8.5	−8.1	−39.4
F14	Apigenin	−6.4	−8.2	−8.5	−9.4	−8.5	−41.0
F15	Tricin	−5.8	−6.7	−9.3	−8.6	−7.4	−37.8

number of individual components varied across different periods, as evidenced in Figure 10. Notably, the content of P5 (methyl caffeate), P6 (chlorogenic acid methyl ester), P8 (4-*O*-caffeoylquinic acid), and P10 (caffeic acid) was at its lowest during the S3 period, while the content of P4 (3,4-dihydroxybenzoic acid) and P8 (4-*O*-caffeoylquinic acid) peaked during the S6 period. Chlorogenic acid is a phenylpropanoid substance formed by the shikimic acid pathway through the activity of phenylalanine ammonia-lyase, whereas caffeic acid serves as an important precursor substance in the synthesis process. Interestingly, the variation in caffeic acid content depicted in Figure 10 exhibits an opposing trend to that of chlorogenic acid, indicating a potential connection between this outcome and chlorogenic acid synthesis. Compared to

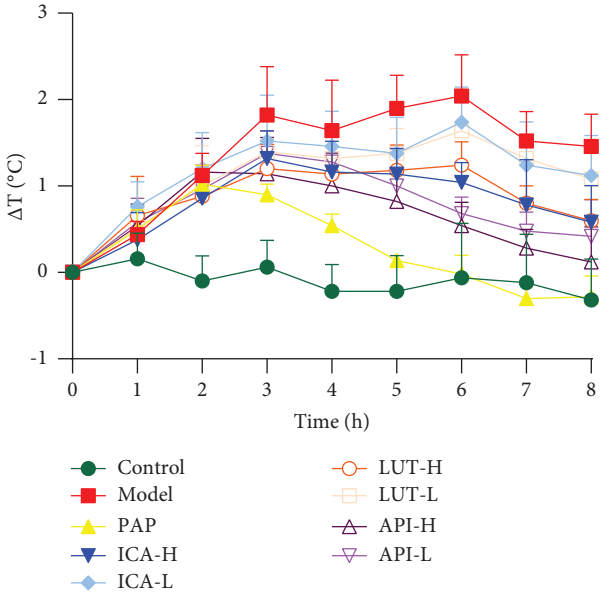

Figure 6: Antipyretic activity of three components in mice. Note: PAP, paracetamol; ICA-H (-L), high (low) dose group of 3,5-*O*-dicaffeoylquinic acid; LUT-H (-L), high (low) dose group of luteolin-7-*O*-glucoside; API-H (-L), high (low) dose group of apigenin-7-*O*-glucoside.

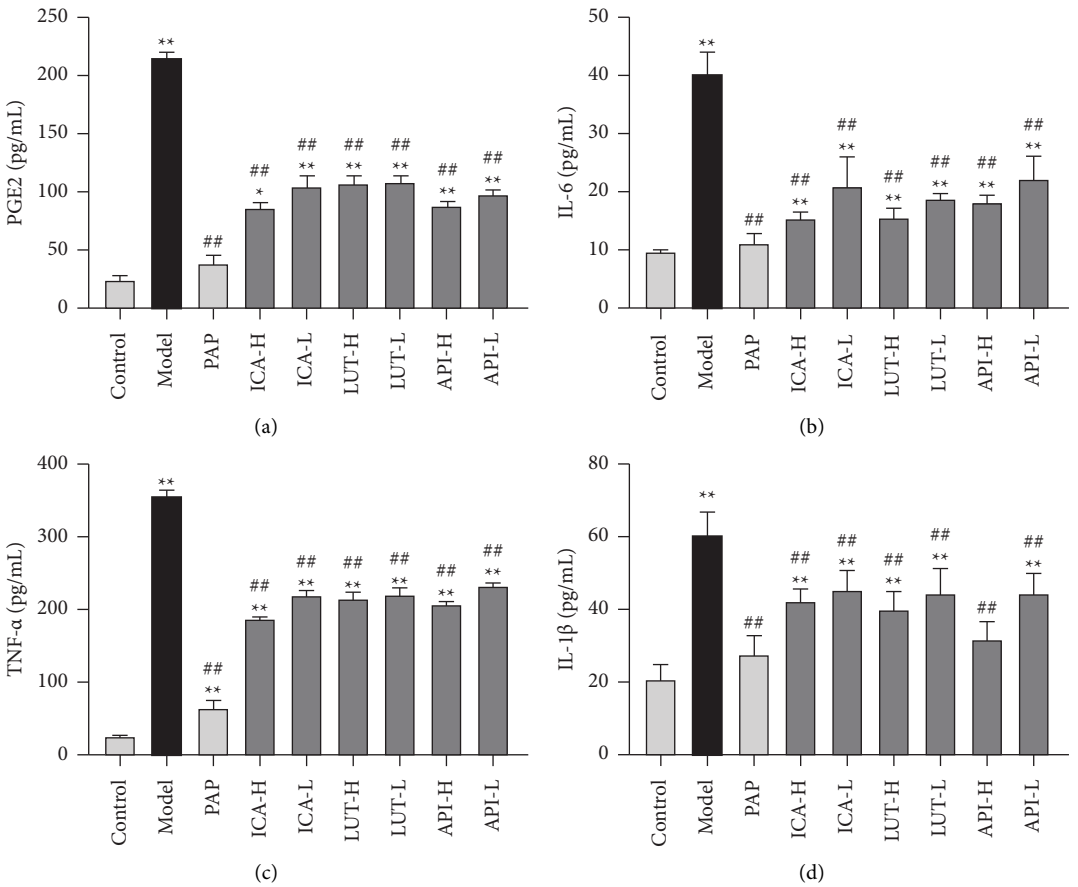

Figure 7: Effect of three components on the levels of endogenous pyrogen and febrile mediators.

Table 2: Regression equation, detection limit, quantification limit, repeatability, precision, stability, and sample recovery rate of quantitative components.

No.	Calibration curve	R^2	Linearity range (μg/mL)	LOD (ng/mL)	LOQ (ng/mL)	Repeatability	Precision		Stability	Recovery	
						RSD (%)	Intraday RSD (%)	Interday RSD (%)	RSD (%)	Original (%)	RSD (%)
P1	$y = 6662.6x + 5980.2$	0.9998	0.5950-23.8000	0.50	1.68	1.58	0.98	0.99	1.75	100.17	0.83
P2	$y = 10927x + 571.11$	0.9992	0.3875-15.5000	0.53	1.76	1.76	0.46	0.83	1.96	99.94	0.73
P3	$y = 3886.2x + 750.51$	0.9997	0.2650-10.6000	0.52	1.74	1.43	0.59	0.95	1.77	100.34	1.11
P4	$y = 1981.6x + 281.4$	0.9992	0.0216–0.8630	0.37	1.24	1.75	0.78	3.44	2.15	100.36	2.16
P5	$y = 2271.9x + 189.6$	0.9995	0.0128–0.5130	0.37	1.24	1.67	0.98	2.11	2.87	100.20	2.82
P6	$y = 3030.5x + 171.1$	0.9997	0.0116–0.4630	0.46	1.52	1.89	1.21	2.35	1.96	99.77	2.46
P7	$y = 2100.2x + 139.6$	0.9992	0.0750–3.0000	0.50	1.68	1.45	0.65	2.01	1.94	100.04	1.19
P8	$y = 796.4x + 123.6$	0.9993	0.1131–4.5250	0.49	1.64	1.65	0.57	2.91	1.87	99.92	0.50
P9	$y = 718.73x + 112.92$	0.9998	0.4525-18.1000	0.52	1.74	1.43	0.88	3.32	2.32	99.77	0.99
P10	$y = 3301.8x + 130.6$	0.9991	0.0113–0.4500	0.38	1.28	1.64	0.78	3.27	1.88	99.34	0.42
P11	$y = 790.51x + 38.4$	0.9998	0.0069–0.2750	0.50	1.68	1.85	0.89	1.72	2.09	98.58	2.63
P12	$y = 4491.6x + 81.3$	0.9996	0.0026–0.1050	0.38	1.28	1.35	1.32	2.05	2.87	102.14	1.89
F1	$y = 3269.9x + 1928.8$	0.9990	0.2452-49.0447	0.57	1.91	2.92	2.98	3.31	3.47	98.41	3.05
F2	$y = 10869x + 569.38$	0.9997	0.0339–6.7830	0.10	0.34	1.44	1.78	2.48	0.77	103.40	1.01
F3	$y = 6888.2x + 4159.7$	0.9994	0.1228-24.5568	0.33	1.10	3.02	2.52	3.26	2.81	96.91	1.42
F4	$y = 5228.3x + 4981.8$	0.9994	0.1185-23.7092	0.13	0.45	2.58	1.87	2.74	2.01	99.03	1.03
F5	$y = 2404.9x + 2990.9$	0.9995	0.2136-42.7217	0.38	1.26	1.99	1.69	1.44	2.89	92.80	2.34
F6	$y = 6499.5x + 81.474$	1	0.0533-10.6518	0.09	0.28	1.06	0.16	1.12	1.15	102.10	1.18
F7	$y = 23410x + 21.278$	1	0.0099–1.9803	0.02	0.06	0.57	0.34	1.13	0.75	107.40	1.53
F8	$y = 4099x + 55.215$	0.9997	0.0095–1.9050	0.06	0.21	1.04	1.38	2.20	1.61	94.28	1.81
F9	$y = 10296x + 541.59$	0.9997	0.0358–7.1690	0.27	0.90	1.53	1.27	3.03	3.20	98.19	0.46
F10	$y = 3363.5x + 41.835$	0.9999	0.0137–2.7367	0.08	0.26	0.92	1.03	1.84	2.25	103.60	1.17
F11	$y = 7915.4x + 2129.1$	0.9993	0.0997-19.9367	0.16	0.55	3.01	2.97	3.71	3.38	103.80	3.04
F12	$y = 2694.1x + 19.246$	0.9994	0.0044–0.8891	0.03	0.11	1.46	3.17	3.19	1.74	101.00	2.55
F13	$y = 32037x - 27.074$	1	0.0017–0.3481	0.01	0.04	2.97	2.14	3.01	2.80	97.31	2.54
F14	$y = 579.2x - 3.4908$	1	0.0064–1.2717	0.09	0.29	0.55	0.74	2.24	1.79	95.99	1.04
F15	$y = 15697x + 34.838$	0.9999	0.0045–0.8975	0.04	0.12	1.46	1.09	1.13	2.38	103.80	2.01

Note. The components corresponding to the numbers in the table are the same as in Table 1.

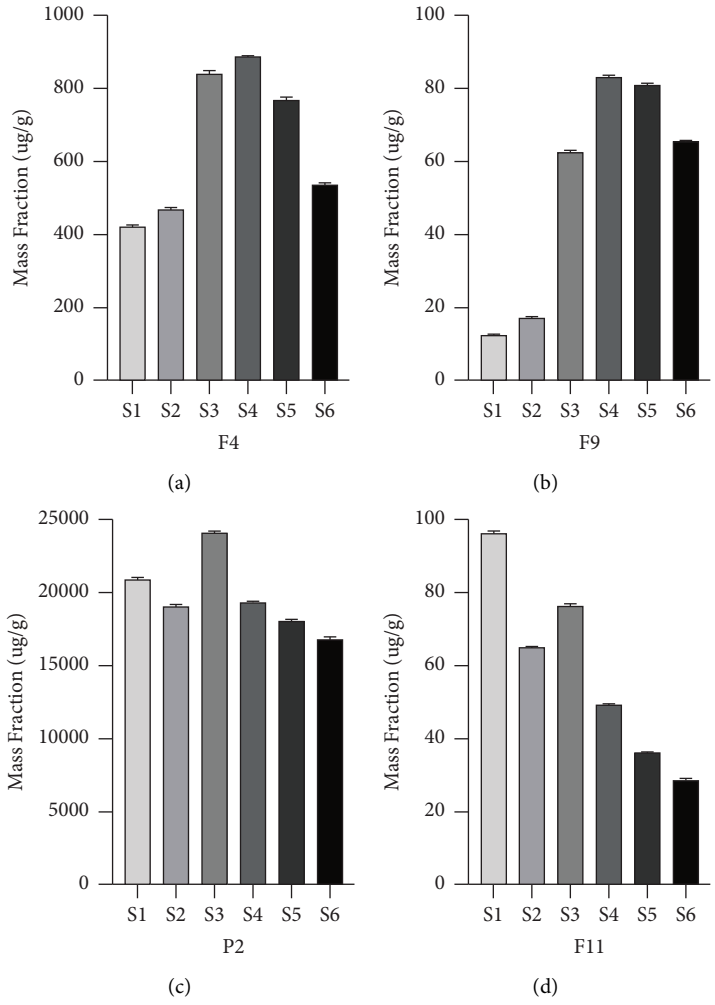

Figure 8: The content change of the four components.

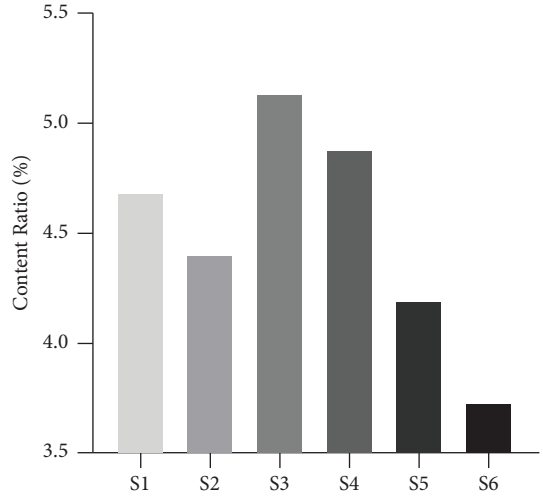

Figure 9: The content ratio of different components in different developmental periods.

phenolic acids, the distribution of flavonoids was more consistent, with most flavonoids demonstrating higher content during the S3 period.

3.9.2. Comparative Analysis of Phenolic Acid Quality Control Components in LJF. In addition to 3,5-*O*-dicaffeoylquinic acid, chlorogenic acid and 4,5-*O*-dicaffeoylquinic acid were

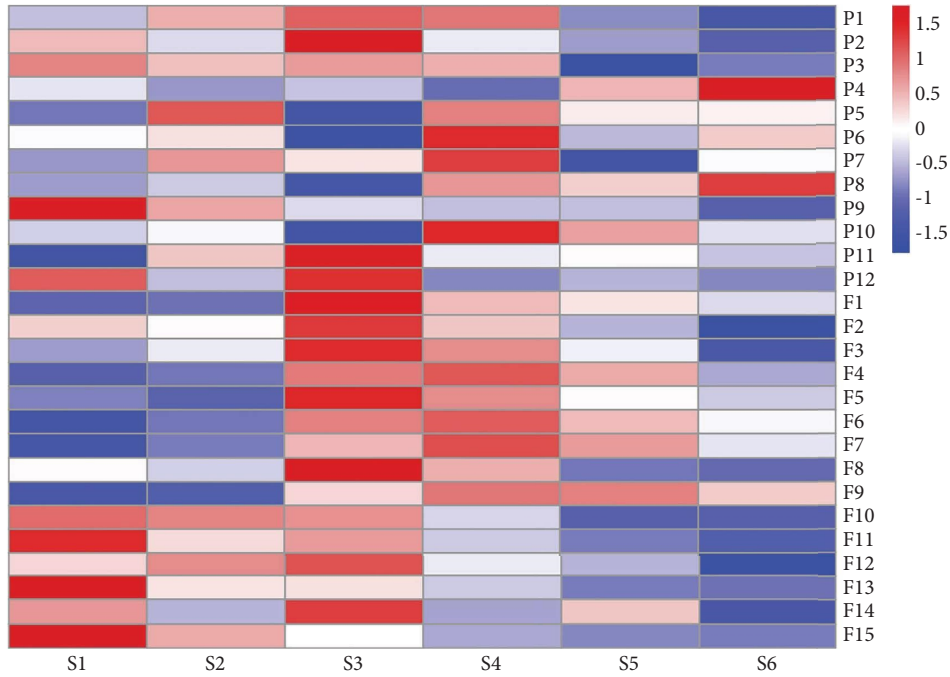

Figure 10: The content of phenolics at different periods. Note: the content data of different components have been standardized by *Z*-score.

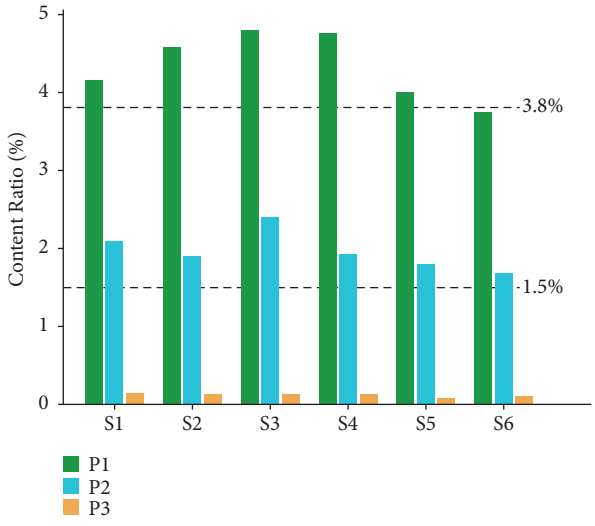

Figure 11: The content ratio of three phenolic acid quality control components. Note: P1, chlorogenic acid; P2, 3,5-*O*-dicaffeoylquinic acid; P3, 4,5-*O*-dicaffeoylquinic acid.

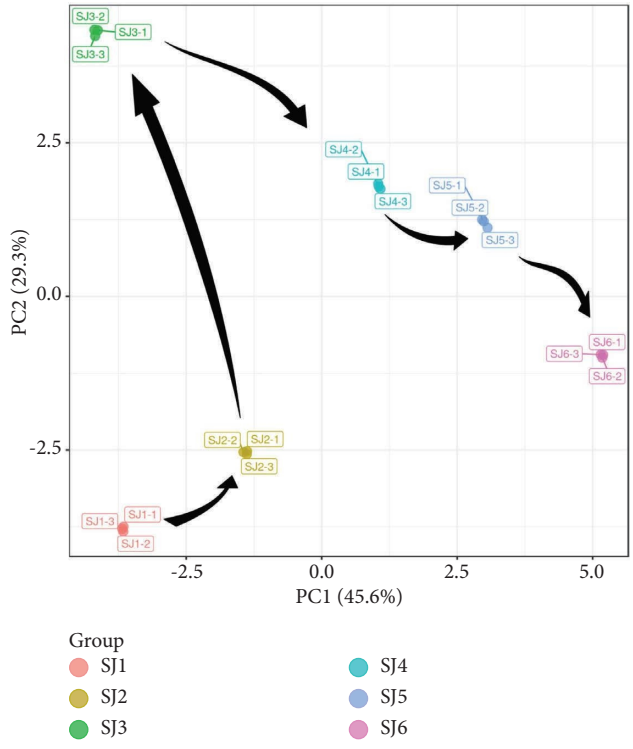

Figure 12: PCA score scatter plot.

also quality control components of LJF. We plot the contents of the above three acids in Figure 11. The chlorogenic acid content of the sample in this study reached the content standard of 1.5%, and five periods of the sample reached the standard of 3.8% phenolic acid component stipulated by pharmacopeia. Therefore, there was a certain contradiction between the high chlorogenic acid content and the quality standard of phenolic acid stipulated by the pharmacopeia of LJF. If the chlorogenic acid content of LJF was up to the standard (≥1.5%), the content of the other two phenolic acids was of little significance. Even if the two phenolic acids were not contained in the medicine, this batch met LJF pharmacopeia standards. In different developmental periods of LJF, 3,5-*O*-dicaffeoylquinic acid content accounted for 0.408~0.505% of the chlorogenic acid content and 4,5-*O*-dicaffeoylquinic acid content accounted for 0.023~0.038% of the chlorogenic acid content. When the chlorogenic acid

reached the standard of 1.5%, the content of 3,5-*O*-dicaffeoylquinic acid was 0.612~0.758% and 4,5-*O*-dicaffeoylquinic acid content was 0.035~0.057%. Therefore, the total acid content was 1.931~2.043%, far from the standard of 3.8% stipulated by the pharmacopeia. As the previous study pointed out, 3,5-*O*-dicaffeoylquinic acid was crucial to the antipyretic effect of LJF, so its content standard should be strictly controlled. However, the current LJF quality standard has defects in the control of 3,5-*O*-dicaffeoylquinic acid content. The total acid content of LJF includes chlorogenic acid, which accounted for 0.648~0.695%. However, when the total acid content reached 3.8%, the content of chlorogenic acid in LJF was about 2.462~2.641%, much higher than the standard of 1.5%.

3.9.3. Multivariate Statistical Analysis. Principal component analysis (PCA) is an unsupervised pattern recognition method. PCA can visually display the data differences in each group through dimensionality reduction of data. Since the antipyretic components of LJF were not consistent in different periods, SIMCA 14.1 software was used to reduce the dimensionality of the data (Figure 12). Figure 12 visually represents the variations between samples. LJF samples at different developmental periods formed a single cluster, while different periods showed a notable separation trend.

PCA is an unsupervised analysis method that has limitations. In-group errors and random errors cannot be ignored or eliminated during analysis. Therefore, supervised orthogonal partial least-squares discriminant analysis (OPLS-DA) is needed to determine the different components of different developmental periods. First, the permutation model was used to verify the fitting degree of the OPLS-DA model. In the positive ion model, the parameters of 200 permutation models were $R^2 = 0.999$ and $Q^2 = 0.999$, indicating that the model was effective and that the differential chemical components could be further identified. The study employed OPLS-DA analysis to detect distinct components in varying developmental periods. Differential components were screened based on VIP >1, and potential differential components of LJF were examined across different periods. The analysis identified 10 components, comprising 8 phenolic acids and 2 flavonoids (Figure 13).

Based on the analysis, phenolic acids exert a more pronounced effect on the differentiation of samples in distinct periods than flavonoids. Specifically, the content difference of phenolic acids in different periods is evident. Therefore, the selection of picking time bears a greater impact on phenolic acids, ultimately resulting in an indirect effect on the antipyretic effect of LJF.

4. Discussion

Using network pharmacology, LJF's phenolic acid and flavonoid active components were analyzed to construct a network of key potential components and potential targets. The study found 186 potential components that act directly on fever targets and may be the key antipyretic components in LJF's efficacy.

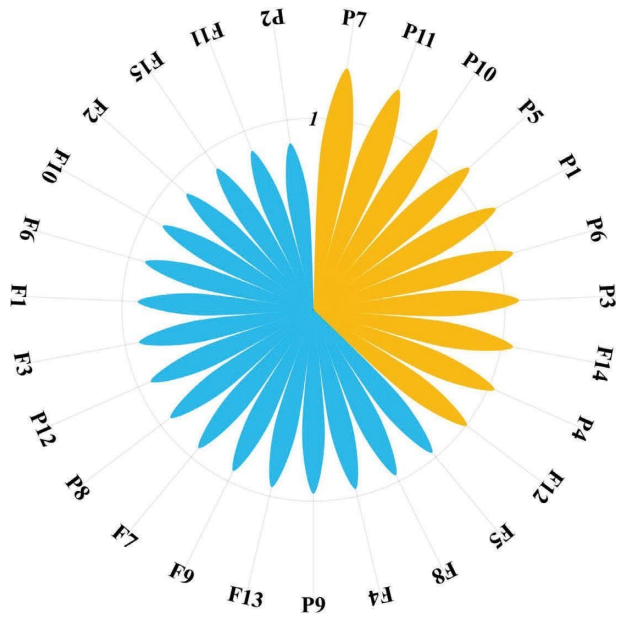

Figure 13: VIP values of phenolic acids and flavonoids in LJF.

In the GO biological process analysis results, the protein phosphorylation showed the greatest enrichment. The process of signal transduction involves reversible phosphorylation of a variety of proteins. Proteins can amplify and transmit signals through reversible phosphorylation and different cascade reactions. In conclusion, protein phosphorylation plays an essential role in cell signaling [44, 45]. Protein serine/threonine/tyrosine kinase activity significantly enriched GO molecular function analysis. It has implications in regulating cell morphology, motility, and cell transformation [46]. Serine/threonine/tyrosine kinase 1 (STYK1) was upregulated in nonsmall cell lung cancer (NSCLC) and correlated with poor clinical outcomes. Moreover, STYK1 hindered forkhead box O1 actions, prompting metastasis and epithelial-mesenchymal transition in NSCLC [47]. The cellular components of GO were mainly enriched in membrane rafts, which are fundamental for maintaining cellular functions such as signal transduction [48], receptor activation [49], and intracellular lipid and protein trafficking [50]. Interfering with this process leads to abnormal growth, differentiation, metabolism, and biological traits, resulting in various illnesses.

The lipid and atherosclerosis signaling pathway was closely related to the calcium signaling pathway, NF-kappa B signaling pathway, toll-like receptor signaling, apoptosis, and TNF signaling pathway. As the responder and transmitter of calcium signals, calcium-ion-binding protein plays an essential role in the signaling pathway [51]. Proper regulation of calcium concentration is necessary for systemic metabolism, and disruption of calcium homeostasis is associated with various metabolic diseases in vivo [52]. Inflammation mainly refers to the complex reaction caused by tissue damage or pathogen infection, leading to various inflammatory diseases. TRP channels were a class of ion channels that responded to various chemical and physical stimuli derived from harmful agents and contributed to

increased intracellular cation concentrations [53]. Inflammatory diseases cause TRP ion channels to malfunction [54], increasing calcium influx into the cell [55, 56]. This increase in calcium ion concentration can trigger reactions, including the production and release of arachidonic acid [57] and respiratory burst [58].

The anti-inflammatory responses have been induced by cAMP, and its pathways have been extensively used for treating inflammatory diseases. cAMP is one of the important inflammatory mediators of the central nervous system, a crucial information-conveying molecule in response to external stimuli, and the main positive heating medium in the central nervous system. Increased cAMP content is a common intermediate link in various pyrogen-induced fevers, which can participate in thermoregulation through the endogenous pyrogen-hypothalamic Na^+/Ca^{2+}-cAMP pathway [59–62]. The cAMP-dependent protein kinase signal transduction pathway may be involved in the central pyrogenic mechanisms in rats [63]. Therefore, LJF can exert antipyretic effects via the cAMP signaling pathway. In conclusion, the KGEE analysis indicated that the antipyretic mechanism of phenolic acids and flavonoids in LJF is modulated mainly through regulating these pathways.

The binding energy of phenolic acids and flavonoids in LJF with mPGES-1, EP1, EP2, EP3, and EP4 targets is satisfactory. The four most important components were luteolin-7-*O*-glucoside, apigenin-7-*O*-glucoside, 3,5-*O*-dicaffeoylquinic acid, and luteolin. Luteolin-7-*O*-glucoside and apigenin-7-*O*-glucoside have pharmacological activities to reduce oxidative stress and inflammation. Luteolin-7-*O*-glucoside could inhibit the activation of NF-kappa B and phosphorylation of Akt [64] and significantly reduce the content of cholesterol hydroxylated species such as 7-α-hydroxicholesterol and 7-β-hydroxicholesterol [65]. Apigenin-7-*O*-glucoside could significantly inhibit H_2O_2-induced ROS production in RAW 264.7 cells, free radical-induced oxidative damage on erythrocytes, and LPS-induced NF-kappa B/NLRP3/caspase-1 signaling in RAW 246.7 cells [66]. 3,5-*O*-dicaffeoylquinic acid has shown a protective effect against inflammation-related diseases and attenuated inflammation-mediated pain hypersensitivity by enhancing autophagy by inhibiting MCP3-induced JAK2/STAT3 signaling [67]. Additionally, 3,5-*O*-dicaffeoylquinic had a protective effect against acute lung injury caused by LPS in mice [68]. Luteolin reduced the expression of proinflammatory molecules (TNF-α, ICAM-1) in vivo [69] and inhibited LPS-induced IL-6 production in the brain by inhibiting the JNK signaling pathway and activation of AP-1 in microglia [70]. In addition, luteolin exhibited anti-inflammatory activity at micromolar concentrations [71], indicating its potential as a promising component for further development. Binding to an EP receptor on the cell membrane is essential for PGE2 to exert its biological work. The EP1 receptor activates protein kinase C by upregulating intracellular Ca^{2+} while partially coupled to G protein Gαs. The EP2 receptor activates the PKA pathway by increasing intracellular cAMP levels and partially coupling to G protein Gαs [72]. The docking results showed that LJF components were well connected to EP1 and EP2 receptors. The results of the KEGG analysis also indicated that the calcium signaling and cAMP signaling pathways were the main antipyretic pathways of LJF. Therefore, it was hypothesized that LJF's antipyretic mechanism involves interaction between its main antipyretic components and PGE2 receptors. This interaction regulates calcium signaling, cAMP signaling, and other pathways, ultimately resulting in antipyretic effects.

Yeast-induced pyrexia by increasing prostaglandin synthesis is a useful model for screening drugs for their antipyretic effect [73]. Combined with previous experiments, we found that LPS-induced body temperature changes were susceptible to ambient temperature and manipulation stimuli. In contrast, yeast-induced fever was more stable and persistent. Therefore, the yeast heating model was selected for the experiment. In the present study, intraperitoneal administration of three components (high-low dose), especially API-H, significantly attenuated the rectal temperature of yeast-induced febrile mice. In addition, we tested the effect of three components on PGE2, IL-6, TNF-α, and IL-1β secretion by yeast-induced pyretic animals. IL-6, TNF-α, and IL-1β are important endogenous pyrogen, which can directly or indirectly cause the release of PGE2 and increase body temperature [42, 43]. The data showed that three high- and low-dose components reduced the endogenous pyrogen or febrile mediator levels in febrile mice. Therefore, it is reasonable to choose 3,5-*O*-dicaffeoylquinic acid and luteolin-7-*O*-glucoside as the quality control components of LJF in the Chinese pharmacopeia.

Using molecular docking, LJF's antipyretic properties were analyzed and several related phenolic acids and flavonoids were identified. Consequently, changes in the content of these components can serve as an indirect indicator of LJF's antipyretic effect. According to the proportion of each component content in different developmental periods of LJF, the antipyretic effect of LJF in S3 and S4 was better than that in other periods, suggesting that the harvesting period of the LJF should not be too early. By discussing the content of three phenolic acids in LJF, defects in quality control of LJF in Chinese Pharmacopoeia were detected. The "Siji Hua" germplasm of LJF had an individual problem, while other germplasms had a general problem. The main antipyretic component, 3,5-*O*-dicaffeoylquinic acid, has a relatively loose restriction condition, which affects the efficacy of LJF. The LJF total acid content standard ≥3.8% specified in the 2020 Chinese Pharmacopoeia needs to be discussed. Quality control of phenolic acid components should be increased to ensure the quality of LJF, as the picking time significantly influences these components.

5. Conclusion

This paper investigated the antipyretic mechanism of LJF's phenolic acids and flavonoids using network pharmacology and molecular docking technology, providing a modern scientific explanation of the curative effect of traditional heat-clearing and detoxification of LJF. 3,5-*O*-dicaffeoylquinic acid, luteolin-7-*O*-glucoside, and apigenin-7-*O*-glucoside were found to have

significant antipyretic activity in a yeast-induced pyrexia model. The ESI-QqQ-MS/MS method analyzed antipyretic components to guide LJF's quality control. However, more research is necessary to explore the molecular mechanism and develop new drugs.

Data Availability

The data supporting the findings of the study included within the article or supplementary materials.

Additional Points

Sample Availability: samples are not available from the authors.

Conflicts of Interest

The authors declare that they have no conflicts of interest.

Authors' Contributions

Lewen Xiong, Wenjing Huang, and Yan Liu developed the methodology; Lewen Xiong and Yang Wang performed the software analysis; Yan Liu, Ying Jin, and Hongwei Zhao validated the manuscript; Lewen Xiong prepared the original draft of the manuscript; Lewen Xiong, Longfei Zhang, and Yongqing Zhang reviewed and edited the manuscript. All authors have read and agreed to the published version of the manuscript. Lewen Xiong and Wenjing Huang contributed equally to this work.

Acknowledgments

This research was funded by the Major Scientific and Technological Innovation Projects in Shandong Province (2019JZZY011020), National Key Research and Development Program of China (2017YFC1701503), and Shandong Natural Science Foundation Project (ZR2021QH238).

Supplementary Materials

Supplementary Table 1: information and HPLC-MS/MS parameters for MRM on phenolic acids and flavonoids in LJF. Supplementary Table 2: phenolic acids and flavonoids in LJF. Supplementary Table 3: contents of phenolic acids and flavonoids in LJF at different developmental periods. Supplementary Figure 1: MS chromatogram of the LJF extract. (*Supplementary Materials*)

References

[1] Chinese Pharmacopoeia Commission, *ChP 2020*, China Medical Science Press, Beijing, China, 2020.

[2] X. Shang, H. Pan, M. Li, X. Miao, and H. Ding, "*Lonicera japonica* Thunb.: ethnopharmacology, phytochemistry and pharmacology of an important traditional Chinese medicine," *Journal of Ethnopharmacology*, vol. 138, pp. 1–21, 2011.

[3] L. Wang, Q. Jiang, J. Hu, Y. Zhang, and J. Li, "Research progress on chemical constituents of Lonicerae japonicae flos," *BioMed Research International*, vol. 2016, Article ID 8968940, 18 pages, 2016.

[4] R. Yan, Y. Zhang, Y. Li, L. Xia, Y. Guo, and Q. Zhou, "Structural basis for the recognition of SARS-CoV-2 by full-length human ACE2," *Science*, vol. 367, no. 6485, pp. 1444–1448, 2020.

[5] L. Ge, H. Wan, S. Tang et al., "Novel caffeoylquinic acid derivatives from *Lonicera japonica* Thunb. flower buds exert pronounced anti-HBV activities," *The Royal Society of Chemistry Advances*, vol. 8, no. 62, pp. 35374–35385, 2018.

[6] Z. Lou, H. Wang, S. Zhu, C. Ma, and Z. Wang, "Antibacterial activity and mechanism of action of chlorogenic acid," *Journal of Food Science*, vol. 76, no. 6, pp. M398–M403, 2011.

[7] G. Li, X. Wang, Y. Xu, B. Zhang, and X. Xia, "Antimicrobial effect and mode of action of chlorogenic acid on *Staphylococcus aureus*," *European Food Research and Technology*, vol. 238, no. 4, pp. 589–596, 2014.

[8] H. S. Shin, H. Satsu, M. J. Bae, M. Totsuka, and M. Shimizu, "Catechol groups enable reactive oxygen species scavenging-mediated suppression of PKD-NFkappaB-IL-8 signaling pathway by chlorogenic and caffeic acids in human intestinal cells," *Nutrients*, vol. 9, no. 2, p. 165, 2017.

[9] N. Liang and D. D. Kitts, "Chlorogenic acid (CGA) isomers alleviate interleukin 8 (IL-8) production in caco-2 cells by decreasing phosphorylation of p38 and increasing cell integrity," *International Journal of Molecular Sciences*, vol. 19, no. 12, p. 3873, 2018.

[10] S. Huang, L. L. Wang, N. N. Xue et al., "Chlorogenic acid effectively treats cancers through induction of cancer cell differentiation," *Theranostics*, vol. 9, no. 23, pp. 6745–6763, 2019.

[11] Chinese Pharmacopoeia Commission, *ChP 2020*, China Medical Science Press, Beijing, China, 2000.

[12] Chinese Pharmacopoeia Commission, *ChP 2015*, China Medical Science Press, Beijing, China, 2020.

[13] J. Xiong, S. Li, W. Wang, Y. Hong, K. Tang, and Q. Luo, "Screening and identification of the antibacterial bioactive compounds from *Lonicera japonica* Thunb. leaves," *Food Chemistry*, vol. 138, no. 1, pp. 327–333, 2013.

[14] Z. Xu, K. Li, T. Pan et al., "Lonicerin, an anti-algE flavonoid against *Pseudomonas aeruginosa* virulence screened from Shuanghuanglian formula by molecule docking based strategy," *Journal of Ethnopharmacology*, vol. 239, Article ID 111909, 2019.

[15] J. H. Lee and Y. Han, "Antiarthritic effect of lonicerin on Candida albicans arthritis in mice," *Archives of Pharmacal Research*, vol. 34, no. 5, pp. 853–859, 2011.

[16] A. P. Rogerio, A. Kanashiro, C. Fontanari et al., "Anti-inflammatory activity of quercetin and isoquercitrin in experimental murine allergic asthma," *Inflammation Research*, vol. 56, no. 10, pp. 402–408, 2007.

[17] X. Li, Q. Jiang, T. Wang, J. Liu, and D. Chen, "Comparison of the antioxidant effects of quercitrin and isoquercitrin: understanding the role of the 6″-OH group," *Molecules*, vol. 21, no. 9, p. 1246, 2016.

[18] J. Shao, C. Wang, L. Li et al., "Luteoloside inhibits proliferation and promotes intrinsic and extrinsic pathway-mediated apoptosis involving MAPK and mTOR signaling pathways in human cervical cancer cells," *International Journal of Molecular Sciences*, vol. 19, no. 6, p. 1664, 2018.

[19] A. Imani, N. Maleki, S. Bohlouli, M. Kouhsoltani, S. Sharifi, and S. Maleki Dizaj, "Molecular mechanisms of anticancer effect of rutin," *Phytotherapy Research*, vol. 35, no. 5, pp. 2500–2513, 2020.

[20] A. B. Enogieru, W. Haylett, D. C. Hiss, S. Bardien, and O. E. Ekpo, "Rutin as a potent antioxidant: implications for neurodegenerative disorders," *Oxidative Medicine and Cellular Longevity*, vol. 2018, Article ID 6241017, 17 pages, 2018.

[21] Q. Li, Z. Tian, M. Wang et al., "Luteoloside attenuates neuroinflammation in focal cerebral ischemia in rats via regulation of the PPARγ/Nrf2/NF-κB signaling pathway," *International Immunopharmacology*, vol. 66, pp. 309–316, 2019.

[22] M. Ek, D. Engblom, S. Saha, A. Blomqvist, P. J. Jakobsson, and A. Ericsson-Dahlstrand, "Inflammatory response: pathway across the blood-brain barrier," *Nature*, vol. 410, no. 6827, pp. 430-431, 2001.

[23] K. Yamagata, K. Matsumura, W. Inoue et al., "Coexpression of microsomal-type prostaglandin E synthase with cyclooxygenase-2 in brain endothelial cells of rats during endotoxin-induced fever," *Journal of Neuroscience*, vol. 21, no. 8, pp. 2669–2677, 2001.

[24] D. Engblom, M. Ek, I. M. Andersson et al., "Induction of microsomal prostaglandin E synthase in the rat brain endothelium and parenchyma in adjuvant-induced arthritis," *Journal of Comparative Neurology*, vol. 452, no. 3, pp. 205–214, 2002.

[25] J. C. Schiltz and P. E. Sawchenko, "Distinct brain vascular cell types manifest inducible cyclooxygenase expression as a function of the strength and nature of immune insults," *Journal of Neuroscience*, vol. 22, no. 13, pp. 5606–5618, 2002.

[26] P. E. Sawchenko and P. E. Sawchenko, "Signaling the brain in systemic inflammation: the role of perivascular cells," *Frontiers in Bioscience*, vol. 8, no. 6, pp. s1321–s1329, 2003.

[27] A. I. Ivanov and A. A. Romanovsky, "Prostaglandin E2 as a mediator of fever: synthesis and catabolism," *Frontiers in Bioscience*, vol. 9, no. 1-3, pp. 1977–1993, 2004.

[28] C. Jegerschold, S. C. Pawelzik, P. Purhonen et al., "Structural basis for induced formation of the inflammatory mediator prostaglandin E2," *Proceedings of the National Academy of Sciences of the U S A*, vol. 105, no. 32, pp. 11110–11115, 2008.

[29] F. Ushikubi, E. Segi, Y. Sugimoto et al., "Impaired febrile response in mice lacking the prostaglandin E receptor subtype EP3," *Nature*, vol. 395, no. 6699, pp. 281–284, 1998.

[30] K. Oka, T. Oka, and T. Hori, "PGE_2 receptor subtype EP_1 antagonist may inhibit central interleukin-1β-induced fever in rats," *American Journal of Physiology- Regulatory, Integrative and Comparative Physiology*, vol. 275, no. 6, pp. R1762–R1765, 1998.

[31] T. Oka, K. Oka, and C. B. Saper, "Contrasting effects of E type prostaglandin (EP) receptor agonists on core body temperature in rats," *Brain Research*, vol. 968, no. 2, pp. 256–262, 2003.

[32] T. Oka, "Prostaglandin E2 as a mediator of fever: the role of prostaglandin E (EP) receptors," *Frontiers in Bioscience*, vol. 9, no. 1-3, pp. 3046–3057, 2004.

[33] F. Ushikubi, M. Hirata, and S. Narumiya, "Molecular biology of prostanoid receptors; an overview," *Journal of Lipid Mediators and Cell Signalling*, vol. 12, no. 2-3, pp. 343–359, 1995.

[34] M. Sheng and M. E. Greenberg, "The regulation and function of c-fos and other immediate early genes in the nervous system," *Neuron*, vol. 4, pp. 477–485, 1990.

[35] L. Xiong, Y. Liu, H. Zhao et al., "The mechanism of chaiyin particles in the treatment of COVID-19 based on network pharmacology and experimental verification," *Natural Product Communications*, vol. 17, no. 8, Article ID 1934578X2211148, 2022.

[36] Y. Zhou, B. Zhou, L. Pache et al., "Metascape provides a biologist-oriented resource for the analysis of systems-level datasets," *Nature Communications*, vol. 10, no. 1, p. 1523, 2019.

[37] M. Kanehisa and S. Goto, "KEGG: kyoto encyclopedia of genes and genomes," *Nucleic Acids Research*, vol. 28, no. 1, pp. 27–30, 2000.

[38] B. Zhu, C. Qian, F. Zhou et al., "Antipyretic and antitumor effects of a purified polysaccharide from aerial parts of Tetrastigma hemsleyanum," *Journal of Ethnopharmacology*, vol. 253, Article ID 112663, 2020.

[39] C. Liu, H. Su, H. Wan et al., "Forsythoside A exerts antipyretic effect on yeast-induced pyrexia mice via inhibiting transient receptor potential vanilloid 1 function," *International Journal of Biological Sciences*, vol. 13, pp. 65–75, 2017.

[40] L. Xiong, H. Zhao, Y. Wang et al., "Study on phenolic acids of Lonicerae japonicae Flos based on ultrahigh performance liquid chromatography-tandem mass spectrometry combined with multivariate statistical analysis," *Journal of Separation Science*, vol. 45, no. 13, pp. 2239–2251, 2022.

[41] W. Huang, L. Xiong, L. Zhang et al., "Study on the change pattern of flavonoid content during the development of different germplasm *Lonicera japonica* Thunb," *Chinese Traditional and Herbal Drugs*, vol. 53, pp. 3156–3164, 2022.

[42] H. O. Brito, F. L. Barbosa, R. C. D. Reis et al., "Evidence of substance P autocrine circuitry that involves TNF-α, IL-6, and PGE2 in endogenous pyrogen-induced fever," *Journal of Neuroimmunology*, vol. 293, pp. 1–7, 2016.

[43] C. A. Dinarello, "Cytokines as endogenous pyrogens," *The Journal of Infectious Diseases*, vol. 179, no. s2, pp. S294–S304, 1999.

[44] S. Tardif, L. Lefievre, C. Gagnon, and J. L. Bailey, "Implication of cAMP during porcine sperm capacitation and protein tyrosine phosphorylation," *Molecular Reproduction and Development*, vol. 69, no. 4, pp. 428–435, 2004.

[45] E. de Lamirande and C. O'Flaherty, "Sperm activation: role of reactive oxygen species and kinases," *Biochimica et Biophysica Acta*, vol. 1784, no. 1, pp. 106–115, 2008.

[46] M. G. Callow, F. Clairvoyant, S. Zhu et al., "Requirement for PAK4 in the anchorage-independent growth of human cancer cell lines," *Journal of Biological Chemistry*, vol. 277, no. 1, pp. 550–558, 2002.

[47] Y. Lai, F. Lin, X. Wang et al., "STYK1/NOK promotes metastasis and epithelial-mesenchymal transition in non-small cell lung cancer by suppressing FoxO1 signaling," *Frontiers in Cell and Developmental Biology*, vol. 9, Article ID 621147, 2021.

[48] I. Koyama-Honda, T. K. Fujiwara, R. S. Kasai et al., "High-speed single-molecule imaging reveals signal transduction by induced transbilayer raft phases," *The Journal of Cell Biology*, vol. 219, 2020.

[49] Y. Shi and H. Ruan, "Toward a membrane-centric biology," *Frontiers in Immunology*, vol. 11, p. 1909, 2020.

[50] A. B. Ouweneel, M. J. Thomas, and M. G. Sorci-Thomas, "The ins and outs of lipid rafts: functions in intracellular cholesterol homeostasis, microparticles, and cell membranes," *Journal of Lipid Research*, vol. 61, no. 5, pp. 676–686, 2020.

[51] H. V. McCue, L. P. Haynes, and R. D. Burgoyne, "The diversity of calcium sensor proteins in the regulation of neuronal function," *Cold Spring Harbor Perspectives in Biology*, vol. 2, no. 8, p. 4085, 2010.

[52] K. L. Marcelo, A. R. Means, and B. York, "The Ca(2+)/calmodulin/CaMKK2 Axis: nature's metabolic CaMshaft,"

Trends in Endocrinology and Metabolism, vol. 27, no. 10, pp. 706–718, 2016.

[53] S. Partida-Sanchez, B. N. Desai, A. Schwab, and S. Zierler, "Editorial: TRP channels in inflammation and immunity," *Frontiers in Immunology*, vol. 12, Article ID 684172, 2021.

[54] P. Holzer, "Transient receptor potential (TRP) channels as drug targets for diseases of the digestive system," *Pharmacology & Therapeutics*, vol. 131, no. 1, pp. 142–170, 2011.

[55] X. Zhu, M. Jiang, M. Peyton et al., "trp, a novel mammalian gene family essential for agonist-activated capacitative Ca2+ entry," *Cell*, vol. 85, no. 5, pp. 661–671, 1996.

[56] K. Kiselyov, X. Xu, G. Mozhayeva et al., "Functional interaction between InsP3 receptors and store-operated Htrp3 channels," *Nature*, vol. 396, no. 6710, pp. 478–482, 1998.

[57] E. Krump, M. Pouliot, P. H. Naccache, and P. Borgeat, "Leukotriene synthesis in calcium-depleted human neutrophils: arachidonic acid release correlates with calcium influx," *Biochemical Journal*, vol. 310, no. 2, pp. 681–688, 1995.

[58] D. Granfeldt, M. Samuelsson, and A. Karlsson, "Capacitative Ca2+ influx and activation of the neutrophil respiratory burst. Different regulation of plasma membrane- and granule-localized NADPH-oxidase," *Journal of Leukocyte Biology*, vol. 71, no. 4, pp. 611–617, 2002.

[59] H. P. Laburn, C. Rosendorff, G. Willies, and C. Woolf, "Proceedings: a role for noradrenaline and cyclic AMP in prostaglandin E1 Fever," *Journal of Physiology*, vol. 240, no. 2, pp. 49P-50P, 1974.

[60] T. A. Lennie, M. D. Hirvonen, D. O. McCarthy, and R. E. Keesey, "Fever and the acute elevation in whole-body thermogenesis induced by lateral hypothalamic lesions," *Physiology & Behavior*, vol. 58, no. 2, pp. 237–243, 1995.

[61] P. Petrovicky, O. Kadlecova, and K. Mašek, "Mutual connections of the raphe system and hypothalamus in relation to fever," *Brain Research Bulletin*, vol. 7, no. 2, pp. 131–149, 1981.

[62] R. D. Myers, C. W. Simpson, D. Higgins et al., "Hypothalamic Na+ and Ca++ ions and temperature set-point: new mechanisms of action of a central or peripheral thermal challenge and intrahypothalamic 5-HT, NE, PGE1, and pyrogen," *Brain Research Bulletin*, vol. 1, no. 3, pp. 301–327, 1976.

[63] H. Wang, Y. Wang, Y. Qu et al., "The cAMP-mediated protein kinase signal transduction pathway is involved in the pyrogenic effect of CRH in rats," *Chinese Medical Journal*, vol. 114, no. 10, pp. 1064–1067, 2001.

[64] C. M. Park and Y. S. Song, "Luteolin and luteolin-7-*O*-glucoside inhibit lipopolysaccharide-induced inflammatory responses through modulation of NF-*κ*B/AP-1/PI3K-Akt signaling cascades in RAW 264.7 cells," *NUTR RES PRACT*, vol. 7, no. 6, pp. 423–429, 2013.

[65] A. De Stefano, S. Caporali, N. Di Daniele et al., "Anti-inflammatory and proliferative properties of luteolin-7-O-glucoside," *International Journal of Molecular Sciences*, vol. 22, no. 3, p. 1321, 2021.

[66] W. Wang, R. F. Yue, Z. Jin et al., "Efficiency comparison of apigenin-7-O-glucoside and trolox in antioxidative stress and anti-inflammatory properties," *Journal of Pharmacy and Pharmacology*, vol. 72, no. 11, pp. 1645–1656, 2020.

[67] J. Park, Y. Kim, C. Lee, and Y. T. Kim, "3,5-Dicaffeoylquinic acid attenuates microglial activation-mediated inflammatory pain by enhancing autophagy through the suppression of MCP3/JAK2/STAT3 signaling," *Biomedicine & Pharmacotherapy*, vol. 153, Article ID 113549, 2022.

[68] Y. L. Chen, T. L. Hwang, H. P. Yu et al., "Ilex kaushue and its bioactive component 3,5-dicaffeoylquinic acid protected mice from lipopolysaccharide-induced acute lung injury," *Scientific Reports*, vol. 6, no. 1, Article ID 34243, 2016.

[69] A. Kotanidou, A. Xagorari, E. Bagli et al., "Luteolin reduces lipopolysaccharide-induced lethal toxicity and expression of proinflammatory molecules in mice," *American Journal of Respiratory and Critical Care Medicine*, vol. 165, no. 6, pp. 818–823, 2002.

[70] S. Jang, K. W. Kelley, and R. W. Johnson, "Luteolin reduces IL-6 production in microglia by inhibiting JNK phosphorylation and activation of AP-1," *Proceedings of the National Academy of Sciences of the U S A*, vol. 105, no. 21, pp. 7534–7539, 2008.

[71] G. Seelinger, I. Merfort, and C. M. Schempp, "Anti-oxidant, anti-inflammatory and anti-allergic activities of luteolin," *Planta Medica*, vol. 74, no. 14, pp. 1667–1677, 2008.

[72] S. Y. Cheng, H. Zhang, M. Zhang et al., "Prostaglandin E2 receptor EP2 mediates Snail expression in hepatocellular carcinoma cells," *Oncology Reports*, vol. 31, no. 5, pp. 2099–2106, 2014.

[73] S. Jan and M. R. Khan, "Antipyretic, analgesic and anti-inflammatory effects of Kickxia ramosissima," *Journal of Ethnopharmacology*, vol. 182, pp. 90–100, 2016.